Identification of shallow-donor impurity states in GaAs/GaAlAs multi-quantum wells in moderate magnetic fields

1991 J. Phys.: Condens. Matter 3 8605

(http://iopscience.iop.org/0953-8984/3/44/007)

J. Phys.: Condens. Matter 3 (1991) 8605–8618. Printed in the UK

Identification of shallow-donor impurity states in GaAs/GaAlAs multi-quantum wells in moderate magnetic fields

J L Dunn and E Pearl
Physics Department, The University, Nottingham NG7 2RD, UK

Received 10 May 1991, in final form 9 July 1991

Abstract. Far infrared photoconductivity experiments have recently been reported on silicon-doped GaAs/GaAlAs multi-quantum well structures in magnetic fields of up to 8 T. The resulting spectra contain peaks which can be identified with transitions from the ground state to several higher excited states of a confined Si impurity. In this paper, details of a theoretical model are given which allow these transition energies to be predicted. The model is firstly used to determine transitions to states which are truly bound in the weak field limit. A set of hydrogen-like basis states is constructed in which the exponentials are expanded in terms of Gaussian-type functions in order to introduce some of the Landau-like behaviour required for large fields. Approximate eigenstates are then determined using a numerical diagonalization procedure. The possibility of transitions to states with $m = 2$ is investigated, and mixing between basis states of different parity is allowed for in the case of impurities which are not located at the centre of a quantum well. These results are then used to determine the energies of so-called metastable states, which do not have a low-field counterpart. Transitions to these states are identified in the observed experimental data.

1. Introduction

There has been much discussion in the literature concerning hydrogen-like shallow-donor impurities in semiconductors, both in the bulk and in multi-quantum wells (MQWs). Far infrared (FIR) photoconductivity experiments have recently been performed on GaAs/GaAlAs MQWs (Grimes *et al* 1990), which allow transitions from the bound 1s-like ground state of such impurities to various excited states to be observed in an applied magnetic field. There is little doubt about the identification of transitions to the $2p_{+1}$- and $2p_{-1}$-like excited states in these experiments. However, the remainder of the transitions have not been conclusively identified at present. The aim of this paper is to develop a theoretical model in which transitions are predicted which fit all of the available experimental data.

The underlying cause of the problems in developing a model for hydrogenic impurities is that for the magnetic fields of up to about 10 T used experimentally, the behaviour of the impurities is intermediate between that obtained using a low-field hydrogenic picture and that of a high-field Landau-type formalism. There is also some doubt as to whether a 3D picture should be used, in which so-called metastable states occur (e.g. Klarenbosch *et al* 1990), or whether a quasi-2D picture is more appropriate (Cheng and McCombe 1990; Cheng *et al* 1990).

0953-8984/91/448605 + 14 $03.50

In this paper, a theoretical model will be developed using the 3D picture. States are used which are principally hydrogen-like, but which incorporate some of the required Landau-like behaviour appropriate to higher fields. An analysis of the number of nodes of the predicted eigenstates in the z-direction will be used as an additional aid to identification of the states. In addition, various metastable states will be identified by combining theoretical results with a careful analysis of the available experimental data. A discussion of the relationships between the 3D and quasi-2D models will also be given.

The model used for the hydrogenic states is based on that of Greene and Lane (1986) and earlier works by the same group, and is an extension of our previous work (Dunn *et al* 1990). The model of Greene and Lane (1986) has been extended to include the effects of higher excited states and of states with angular momentum $m = \pm 2$. It has also been modified to allow for a non-isotropic effective mass, and to include the effects of odd-parity states which are important for impurities which are not located at the centre of a quantum well.

2. The theoretical model

2.1. *Low-field model for hydrogenic states*

When investigating these systems, it is usual to work in dimensionless units appropriate to the systems concerned. For GaAs/GaAlAs MQWs, the unit of length is chosen to be the GaAs effective Bohr radius $a_0 = 98.7$ Å and the unit of energy is the GaAs effective Rydberg $R = 5.83$ meV. The angular momentum l_z is in units of $\hbar$, and a quantity γ is chosen as a dimensionless measure of magnetic field, which is related to the field B in Tesla by the relation $\gamma = 0.15\,B$. Cylindrical coordinates are used with the origin at the centre of a quantum well and with the z-axis defined to be the MQW growth axis. The magnetic field is applied along the z-direction.

In this paper, an anisotropic effective mass is allowed for by defining a parallel effective mass $m_\parallel$ for motion in the x–y plane and a perpendicular effective mass $m_\perp$ for motion in the z-direction. It is then convenient to define relative effective masses $m_r^\perp = m_\perp/m^*$ etc., where $m^* = 0.067\,m_e$ is the usual GaAs effective mass. The effective masses in the GaAlAs barriers may be different to those in the GaAs wells.

Using a 3D picture, the Hamiltonian for a shallow-donor impurity can then be written in the approximate form

$$\mathcal{H} = -(1/m_r)\nabla^2 + (1/m_r^\parallel)(\gamma l_z + \tfrac{1}{4}\gamma^2\rho^2) - 2/r + V_B(z) \tag{2.1}$$

where

$$(1/m_r)\nabla^2 = (1/m_r^\parallel)[(1/\rho)(\partial/\partial\rho)(\rho\,\partial/\partial\rho) + (1/\rho^2)(\partial^2/\partial\varphi^2)] + (1/m_r^\perp)\partial^2/\partial z^2. \tag{2.2}$$

$V_B(z)$ is an energy operator for the square well potential, defined to have the value zero in the wells and a constant value V_0 in the barriers. For $Ga_{1-x}Al_xAs$ MQWs, V_0 is taken to be 60% of the total band gap difference ΔE_g between GaAs and GaAlAs, estimated from the empirical expression (Lee *et al* 1980) $\Delta E_g = (1.155x + 0.37x^2)$ eV (where x is the fractional Al concentration). The position of the impurity electron is $r = [\rho^2 + (z - z_I)^2]^{1/2}$, where z_I specifies the z-coordinate of the impurity nucleus.

Many attempts have been made to solve the Hamiltonian (2.1) for MQWs and the analogous Hamiltonian for the bulk. Although exact analytical solutions cannot be found, a number of different methods have been used to obtain approximate solutions

based on both the low-field limit, where a hydrogenic basis set is approximate, and the high-field limit where a Landau-type description should be employed. A good review of the different approaches for the bulk is given in Zawadzki (1991). Unfortunately, the situation of interest here is intermediate between the two field limits.

Greene and Bajaj (1985) and Greene and Lane (1986) were able to predict the 1s to $2p_{\pm 1}$ energy splittings to a reasonable degree of accuracy using a variational approach in which hydrogenic states were expanded in terms of Gaussian-type basis sets. This has the advantage that, although the states are constructed using a weak-field formalism, the Gaussian behaviour of Landau states is partially incorporated in the wavefunctions, making them more appropriate for larger fields. This basic approach will be developed here, although without resort to a variational procedure.

To a first approximation, the eigenstates ψ of a hydrogenic impurity in a quantum well can be expected to be a product of bulk hydrogen states ψ_{nlm} and states $f(z)$ which are solutions of the standard square well problem, i.e.

$$\psi = f(z)\psi_{nlm} \qquad \text{where } f(z) = \begin{cases} \cos(kz) & \text{in the wells} \\ (A\,e^{\kappa z} + B\,e^{-\kappa z}) & \text{in the barriers.} \end{cases} \tag{2.3}$$

The parameters k, κ, A and B are fixed by ensuring that ψ and $(1/m_r^{\perp})\partial\psi/\partial z$ are continuous across the well boundaries.

The angular momentum operator l_z commutes with the Hamiltonian (2.1), so m must be a good quantum number in this system for all field strengths. For impurities located at the centre of a quantum well, the z-type parity π_z ($=(-1)^{l+m}$) is also a good quantum number (N.B.: the total parity is $(-1)^l$). However, n and l will not be good quantum numbers. Hence, approximate eigenstates of the on-centre MQW problems can be found by taking linear combinations of hydrogenic states with different n- and l-values, but with the same value of m and of π_z. However, for off-centre impurities, the parity π_z is not conserved so it is necessary to allow mixing between the odd and even parity sets of states with a given value of m. This is different to the bulk case, where the z-parity must always be conserved.

According to simple electric dipole selection rules, transitions from the 1s-like ground state are only allowed to states with $m = \pm 1$ for the Faraday configuration used experimentally. For on-centre impurities, transitions will also only be allowed to states with even π_z. However, there is evidence that in the bulk, transitions are weakly observed to both states with $m = 0$ and $m = \pm 2$, as well as to states with odd z-parity, due to various weak perturbation effects (e.g. electric field effects (Stillman *et al* 1971)). Hence, the possibility of transitions to all such states will be investigated here.

In the approach of Greene and Lane (1986), the Slater-type exponential factors $e^{-r/n}$ in the standard hydrogen states for the bulk were expanded in terms of basis sets of Gaussians (Huzinaga, 1965):

$$e^{-r/n} = \sum_i C_i\, e^{-a_i r^2} \tag{2.4}$$

where the C_i and a_i are parameters whose values are determined numerically. A further field-dependent parameter δ was included as an additive factor to the a_i in the Gaussians in ρ to allow for the expected reductions in orbit sizes in the x–y plane as the magnetic field strength increases. Their final choice, which they determined variationally, was $\delta = 0.1\gamma$. The final results presented here are obtained following this choice. However, the results are not very sensitive to the precise value used for this parameter.

A basis set of Gaussian-type functions for the MQW problem is constructed by choosing a set of numbers A_k for each (m, π_z) set from the sets of a_i in the Gaussian expansions for each of the states in that set. The precise values chosen are not important; it is the range of values which most strongly influences the final results.

The hydrogen states in a quantum well are thus assumed to be a linear combination of states ψ_i given by

$$\psi_i = f(z)(z - z_I)^{q_i}\rho^{|m|}\, e^{im\varphi} \exp[-\alpha_i(z - z_I)^2] \exp[-(\beta_i + \delta)\rho^2] \quad (2.5)$$

where q_i is a parity-dependent factor for the state i, defined to be 0 for states with even z-parity and 1 for states with odd z-parity. The parameters α_i and β_i are taken from the sets A_k, with the restriction that, if the A_k are listed in order of magnitude, $\alpha_i = A_k \Rightarrow B_i = A_k$ or $A_{k\pm1}$, i.e. that the arguments of the Gaussians in ρ and $(z - z_I)$ are 'similar' in magnitude. The same set of A_k has been used for $m = 0$ and $m = \pm 1$, following Greene and Lane (1986) rather than Greene and Bajaj (1985), who used a different set for each m, although the differences in the final results are quite small. The number of terms k is chosen to be large enough for the resultant wavefunctions to be good, but small enough for calculations with the states to be manageable. A value for k of 5 or 6 for each (m, π_z) set was taken as a reasonable compromise, which gives a total number of basis states i for each set of $(3k - 2) = 13$ or 16.

The final values are A_k used here for all sets of states are the same as those used by Greene and Lane (1986) for the $m = 0$ and $m = \pm 1$ even parity states, namely 13.4, 2.01, 0.454, 0.123, 0.0324 and 0.00717. Many other sets of A_k covering a similar range of values have also been investigated, and found to give very similar results, at least for the lower-lying states. (This included finding precise parameters for the Gaussian expansions by writing a fitting routine to equate the energies of Gaussian and Slater-type states for states such as 3d, which were not considered by Huzinaga (1965).) States with $(m = 2, \pi_z = -1)$ were not considered in the calculations.

Approximate eigenvalues and eigenstates of the Hamiltonian $\mathcal{H}$ can now be found by calculating the overlaps U_{ij} and matrix elements H_{ij} between each pair of basis states i and j, and numerically solving the generalised eigenvalue problem $\mathcal{H}\psi = EU\psi$, where U and H are matrices with elements U_{ij} and H_{ij} respectively. In the original papers of Greene and co-workers, the precise eigenstates obtained were optimized by carrying out a variational procedure. Here, their optimal parameters are used as a starting point for the calculations, so that it is not necessary to repeat a strict variational procedure. It is sufficient to change the parameters slightly 'by hand', and observe the effect on the final results. This saves much computing time. The fact that a simple diagonalization procedure is used also greatly simplifies the determination of higher excited states, as all of the states determined will automatically be orthogonal to each other. (The states are obviously not orthogonal to the true ground states, so the accuracy of any excited states will diminish for higher energy states.)

There is no φ-dependence of the U_{ij} or H_{ij} (between states with the same value of m), so that expressions for both can be immediately reduced to double integrals over ρ and z. Furthermore, the integrals for all contributions except that of the Coulomb term $2/r$ are separable in ρ and z, and can be performed analytically. The ρ-integrals give simple numerical factors, whilst the z-integrals involve probability integrals Φ. However, convergence problems occur when evaluating the z-integrals as probability integrals due to the appearance of very large exponential factors multiplying them. It was therefore found that much more reliable results could be obtained by evaluating the z-integrals numerically from their original definitions, after using symmetry arguments

to reduce them to integrals over positive values of z and to halve the integral range for each well and barrier. A total of 29 wells were included in the integrations, although sufficient accuracy can be obtained by considering far fewer wells. The Coulomb contribution was evaluated as a double integral.

2.2. High-field notation

On a 3D model, the states of a hydrogenic impurity can be labelled in the alternative high-field notation (N, m, ν), where N is the principal Landau quantum number, m the usual magnetic quantum number and ν gives the number of nodes of the wavefunction in the z-direction. The z-parity of these states is thus carried entirely by the quantum number ν, i.e. $\pi_z = (-1)^\nu$ (the total parity is $\pi = (-1)^{m+\nu}$). In this notation and according to the electric dipole selection rules, transitions are allowed to the states (N, ± 1, ν even) for the Faraday configuration. Again, transitions will be weakly allowed to states with $m = 0$ and ± 2, and to states with odd ν for off-centre impurities.

In this notation, the states (N, m, ν) exist for all integers $N \geqslant 0$ with $m \leqslant N$. However, only the states with $N = 0$ and with $N = m$ for $N \geqslant 1$ are truly bound, and extrapolate back to the hydrogen-like states in weak fields. It is these states which are predicted by our model in section 2.1. The remaining states are called metastable states, and will be considered in more detail later.

The diagonalization procedure of the model in section 2.1 will produce $(3k - 2)$ states for each (m, π_z) set. However, not all of these states will have a physical meaning. According to the high-field picture, only one truly bound hydrogenic state is allowed with a given value of m and given number of nodes ν. Thus it is necessary to examine the number of nodes of each of the eigenstates predicted and select only the lowest-energy state with a given value of ν for each m. All other states can be discarded.

3. Results and comparison with experiment

3.1. Hydrogenic picture

FIR photoconductivity measurements on $GaAs/Ga_{1-x}Al_xAs$ MQWs have recently been made with fixed laser energies in fields of up to 8 T (Grimes *et al* 1990). The samples studied had an Al concentration of $x = 0.33$, and the wells and barriers were approximately 150 Å wide. The central 50 Å of each well were doped with silicon to a concentration of approximately 1×10^{16} cm^{-3}. Full details of the sample construction and measurement details are given in Grimes *et al* (1990).

In addition, Chang *et al* (1988) give some results of FIR photoconductivity experiments on 138 Å wide wells (with $x = 0.3$) for variable transition energies, and Jarosik *et al* (1985) produce results for 210 Å wide wells. Cheng and McCombe (1990) and Cheng *et al* (1990) also give results of FIR magneto-optical measurements on GaAs/GaAlAs MQW samples with $x = 0.3$ for both 125 Å and 170 Å well widths. (Both of these papers reproduce the same diagram, but the well width for the second sample is stated to be 150 Å in Cheng *et al* (1990). To be consistent with the other data, it appears most likely that the well width is indeed 170 Å as in Cheng and McCombe (1990).) The above data have all been combined to determine, although somewhat approximately, those results which would have occurred with a 150 Å sample.

It should be noted that the $2p_{-1}$ transition is much weaker than the $2p_{+1}$ transition. This is because the magnitude of the matrix element governing the transition is smaller

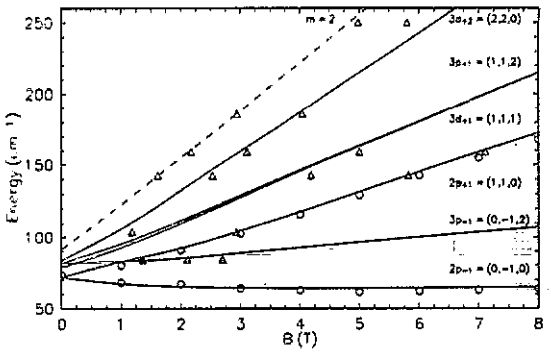

Figure 1. Hydrogenic states: The points Δ are from Grimes *et al* (1990) and the points ○ from Cheng *et al* (1990). The full lines are the results of the theoretical calculations.

(Hasegawa and Howard 1961). The transition is also much broader due to the contributions of off-centre impurities because, as the 1s and $2p_{-1}$ levels are nearly parallel, a small shift in their energy separation will produce large shifts in the magnetic fields at which the photoconductivity peaks occur.

The $2p_{+1}$ and $2p_{-1}$ transitions were fitted to a resonable degree of accuracy by Greene and Lane (1986). However, the theoretical predictions were approximately 3 cm^{-1} higher than the observed data. Also, the $2p_{+1} - 2p_{-1}$ splitting is observed to be slightly less than the value of precisely 2γ which must occur if an isotropic effective mass is used in the calculations. A good fit to the data can be found by choosing slightly larger values for the parallel and perpendicular effective masses. The best fit was found to be with a parallel effective mass $m_{\parallel} = (0.069 \pm 0.001)m_e$ and perpendicular mass $m_{\perp} = (0.068 \pm 0.001)m_e$ for the 150 Å wide wells considered here.

The required transition energies can also be reduced by taking the effective masses in the barriers to be larger than those in the wells. The effective masses in the barriers were thus increased from those in the wells by the additive factor $0.083\, m_e x$ (as used by Greene and Bajaj, 1985), which lowers the 1s to $2p_{+1}$ splitting by approximately 1 cm^{-1}. Results were also obtained with the effective dielectric constant reduced to $(12.53 - 2.73x)$ in the barriers (as used by Fraizzoli *et al* 1990), but this was found to fractionally increase the splitting (by around 0.04 cm^{-1}).

The final results for on-centre impurities are shown in figure 1. Those theoretical predictions which fit the observed experimental data are shown, together with the relevant data points of Grimes *et al* (1990), averaged over all samples. The average data for the $2p_{+1}$ and $2p_{-1}$ transitions as observed by other workers is also shown (see above). The transitions presented are the two lowest $m = \pm 1$ even parity states ($2p_{\pm 1}$ and $3p_{\pm 1}$), the lowest $m = +1$ odd-parity state ($3d_{+1}$) and two $m = +2$ even parity states. The predictions for the $2p_{\pm 1}$ and $3p_{+1}$ states coincide with those predicted by Greene and Lane (1986) when the same parameters are used. The labels here are those which seem most likely from analogy to a pure hydrogen atom, and are given principally for ease of reference. It must be remembered that m is the only label which strictly speaking has a true meaning.

It is generally accepted that the correspondences to the $2p_{-1}$ and $2p_{+1}$ states in the high-field notation are $(0, \bar{1}, 0)$ and $(1, 1, 0)$ respectively. It has been checked that the eigenstates predicted for both of these states have no nodes in the z-direction out to over

1000 Å away from the centre of the well for the zero-field case. (Although a node appears above this, the wavefunction is extremely small at this distance and hence rather inaccurate. This node is taken to be an artefact of the calculation.) The second state predicted with $m = 1$ and even z-parity is found to have two such nodes at acceptable values of z (around ± 120 Å). Hence this must be the physically allowed state (1, 1, 2), which is usually identified with the $3p_{+1}$ state in weak-field notation. Similarly, the $3p_{-1}$ state is identified as $(0, \bar{1}, 2)$.

The $3d_{+1}$ level has one z-type node, so is associated with the (1, 1, 1) state in high-field notation. Figure 1 shows the predictions for the case of on-centre impurities. Transitions from 1s to states of odd-parity such as $3d_{+1}$ should be forbidden for on-centre impurities. However, they will be allowed for off-centre impurities, and may be weakly allowed for on-centre impurities due to various perturbation effects. Any peak in the spectra due to this line would probably correspond to impurities at a finite value of z_I, with that value determined by the distribution of impurities in the sample, and is thus weakly sample-dependent. The predictions for $3p_{+1}$ and $3d_{+1}$ are almost coincident. The experimental points in this region are observed to behave somewhat differently to those of the other points, having a different line shape and being sensitive to different experimental conditions, which is consistent with these results.

The state labelled $3d_{+2}$ has no nodes in the z-direction, so can be identified with the state (2, 2, 0) in high-field notation. However, the identification of this line can not be made conclusively because the data which fits this line also fits the (2, 1, 0) metastable state (see below), to which transitions are expected to be much stronger than to a $m = 2$ state. The second and third $m = 2$ lines also have no z-nodes for acceptable values of z, so should be discarded, even though the third line appears to fit some of the data. The fourth $m = +2$ state, which lies slightly below the level identified with the (3, 1, 0) metastable state, has two nodes so could be the state (2, 2, 2). However, no clear identifications can be made because transitions to the second $m = 2$ level will be extremely weak due to the selection rules. The third state has been reproduced (as a broken line) on figure 1 for reference.

The two data points between $2p_{+1}$ and $2p_{-1}$ have been fitted by the line $3p_{-1}$, to which transitions are expected to be strong. However, as the $3p_{-1}$ line is nearly parallel to 1s, it can only be observed by one of the laser energies used in the FIR photoconductivity experiments. The evidence for this line is thus not conclusive at present, as there are a number of other lines with $m \leqslant 2$ which could fit this data within the given accuracies. Further experimental investigations are necessary. (The data points should not be joined by a single line, as this does not make sense physically.)

Results have been obtained for finite values of z_I. Generally speaking, the pattern of energy levels predicted is very similar to the on-centre case but with a shift to lower energy. Most of the lower energy transitions are ~3 to 5 cm^{-1} lower than the corresponding on-centre cases for $z_I = 20$ Å and 20 to 30 cm^{-1} lower for $z_I = 50$ Å.

3.2. The high-field picture

3.2.1. Metastable states. Further experimental points have been observed which can not be fitted to states derived from a hydrogenic model. It is well known in bulk GaAs that transitions are seen to the metastable states (e.g. Klarenbosch *et al* 1990). Hence, it is likely that transitions to metastable states will also occur in MQWs. One characteristic

feature of transitions to metastable states is that lines occur in pairs separated by the cyclotron resonance energy $\hbar\omega_c$ ($=2\gamma$) or multiples thereof. In particular,

$$E(N, m, \nu) - E(N - m, -m, \nu) = m\hbar\omega_c \tag{3.1}$$

where $E(N, m, \nu)$ is the energy of the state (N, m, ν). The observed data does indeed have several pairs of states with $\hbar\omega_c$ separations. On a 3D hydrogenic picture, there is no fundamental reason why any pairs of states other than nl_{+1} and nl_{-1} should be separated by $\hbar\omega_c$, and it is unlikely that all of the higher-energy states observed which obey this pattern are associated with $m = -1$, as these levels tend to be much lower in energy.

Unfortunately, expressions for the metastable states are not generally known. Numerical expressions have been obtained for the bulk (Simola and Virtamo, 1978), but they are difficult to use in subsequent calculations. Our hydrogenic states, although modified to include Landau-like behaviour, do not model the metastable states in any way. However, a qualitative attempt can be made to identify some of the metastable states.

In bulk, the $(1, -1, 0)$ metastable state has been identified just above and almost parallel to the $2p_{+1}$ level (Narita and Miyao 1971, Wagner and Prettl 1988, Klarenbosch *et al* 1990). A similarly placed level occurs in the quantum well case, so this is identified with the $(1, -1, 0)$ metastable state. The $(2, 1, 0)$ metastable state can then be identified $\hbar\omega_c$ above this (from equation (3.1)). As mentioned above, this latter line coincides with the position of the $(2, 2, 0)$ hydrogenic state. The experimental observations near this point could be a composite of both lines, although the metastable contribution can be expected to dominate due to the electric dipole selection rules.

As the Coulomb potential is rotationally symmetric, it can not mix together Landau states with different values of m. The number of nodes ν must also be conserved. However, states with different Ns will be mixed together. The effect is to increase the separation of the states (N, m, ν) and $(N + 1, m, \nu)$ from $\hbar\omega_c$ to a value $k\hbar\omega_c$, where k is slightly greater than 1 and is approximately constant (decreasing slightly with increasing N and increasing field). As the positions of the $(1, 1, 0)$ and $(2, 1, 0)$ lines have already been identified, this allows the positions of the $(3, 1, 0)$ and $(4, 1, 0)$ metastable states to be determined. The position of the $(2, \bar{1}, 0)$ metastable state can then be fixed by further use of (3.1). The results for all of the metastable states identified are shown in figure 2, together with the experimental data of Grimes *et al* (1990) not shown on figure 1. It can be seen that the agreement between experiment and theory is good.

Cheng *et al* (1990) and Cheng and McCombe (1990) report a line $\hbar\omega_c$ above the $2p_{+1}$ level, and a further line $\hbar\omega_c$ above this. These lines have not been identified using our 3D model, although it is possible that these lines are due to a pair of metastable states, and that the placement of the lowest one $\hbar\omega_c$ above $2p_{+1}$ is somewhat accidental. Further work will be necessary to conclusively identify these states. It should be noted that there is no evidence of the lower of these lines in the data of Grimes *et al* (1990), and the spectra of Cheng *et al* (1990) and Cheng and McCombe (1990) do not appear to be clear in this region, with evidence for further structure.

3.2.2. Landau levels. It is well known that the energies of the free-electron Landau levels are

$$E_N = k^2 + (N + \tfrac{1}{2})\hbar\omega_c. \tag{3.2}$$

In addition, the positions of these Landau levels have also been estimated using the

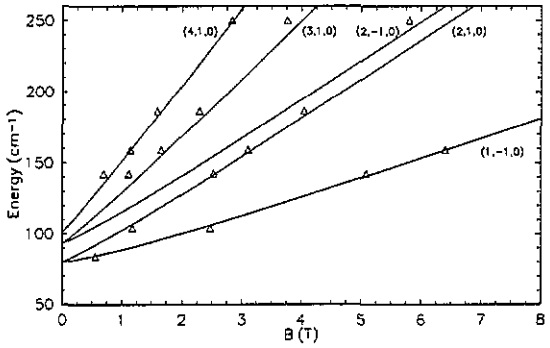

Figure 2. Metastable states: The points Δ are from Grimes *et al* (1990) and the full and broken lines are the results of the theoretical calculations.

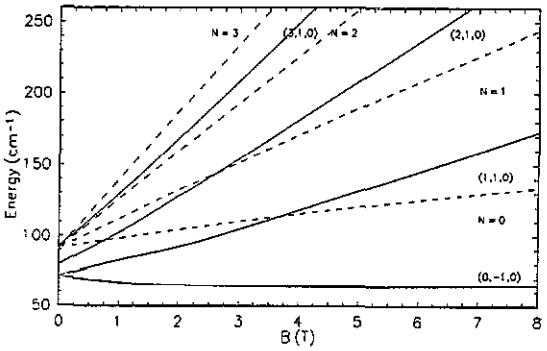

Figure 3. The lowest three Landau levels are shown by the broken lines. Some of the hydrogenic and metastable states from figures 1 and 2 have been reproduced for comparison.

same computer program as that used to calculate the hydrogenic states, but neglecting the contribution of the Coulomb term in the original Hamiltonian. Although the results are not as accurate as those obtained using the formula, they are found to be surprisingly good. The $m = 0$ and $m = -1$ states condense into a narrow band of states around the position of the $N = 0$ Landau level, and the $m = +1$ states into a band of states around the $N = 1$ Landau level. This is precisely as required for the components of the Landau levels which are hydrogenic in origin. (Contributions to the $N = 1$ Landau level from states with $m = 0$ and -1 must be from the metastable states alone (Klarenbosch *et al* 1990).) Although exact degeneracy is not obtained, this illustrates how good the hydrogenic states are at predicting Landau-like behaviour.

The positions of the first few Landau levels calculated using equation (3.2) have been plotted relative to 1s on figure 3, together with some of the hydrogenic and metastable states identified earlier. It is interesting to note that the energy levels of all of the states (N, m, ν) are lower in energy than the Landau level N, and become approximately parallel to the Landau level N in strong fields. This is in common with well known bulk results (Wagner and Prettl 1988) and predictions for the strictly 2D case (MacDonald and Ritchie 1986).

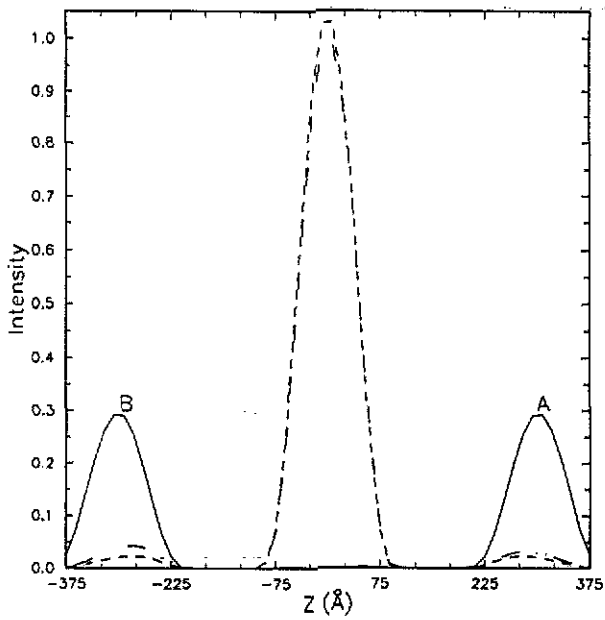

Figure 4. Integrated probability densities for the $2p_{+1}$ states of on-centre impurities (– – –), the $3d_{+1}$ state of on-centre impurities (———) and the $2p_{+1}$ state of impurities with $z_I = 50$ Å (– · · · – · · ·), all in zero field.

3.3. Probability densities

By calculating the probability density as a function of position, it is possible to obtain a physical picture for the behaviour of the impurity electron in its various states. Firstly, it is useful to obtain plots of Ψ^2 integrated over ρ and φ, in order to show the probability of being at a given z-position. This shows that the 1s ground state is almost entirely localized in the central well at all field strengths for 150 Å wide wells. Figure 4 shows the zero-field results for the $2p_{+1}$ and $3d_{+1}$ states of on-centre impurities and the $2p_{+1}$ state with $z_I = 50$ Å in such wells. It can be seen that the $2p_{+1}$ state is strongly localized in the central well, but does extend into next-nearest wells in small fields. In larger fields, the localization in the central well is found to become almost total. In contrast, the odd-parity $3d_{+1}$ wavefunction is very small in the central well and spreads out over several wells. The peak in the second-nearest neighbour wells is approximately half that in the nearest neighbour wells (labelled A and B on the figure). Again this wavefunction becomes much more localised in stronger fields.

It can be seen that for impurities 50 Å away from the centre of a well, the probability of being in both wells A and B has increased compared to the on-centre case. Although the wavefunction would be expected to increase on the side to which the impurity has moved (A), it appears surprising at first that the wavefunction has also increased on the opposite side (B). However, a closer examination of the wavefunctions shows that this is because the states contain some mixing of odd-parity states for the off-centre case, which are much more spread out than the even parity contributions (as shown by the $3d_{+1}$ state on figure 4). Lane and Greene (1986) obtained a similar plot to this but considered even-parity contributions to the states only. Even with this restriction, the

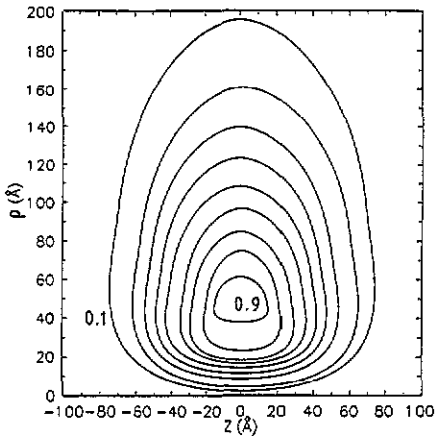

Figure 5. A contour plot of the probability density for the 1s ground state of an on-centre impurity in zero magnetic field. The contours are from 0.1 to 0.9 in steps of 0.1.

size of the wavefunction in well B was almost unaltered by moving the impurity to the well interface. It should be noted that Greene and Lane (1986) find the wavefunction in both wells A and B to be slightly larger than that found here. However, they do not state what well width their calculation is for.

Contour plots of the probability density as a function of z and ρ (integrated over φ) have also been obtained. The result for the 1s ground state of on-centre impurities in zero-field is shown in figure 5. This shows that the electron has highest probability of being about 50 Å from the donor nucleus in the ρ-direction with $z = 0$, i.e. that it is confined to approximately circular orbits in the x–y plane and about the z-axis. Results for the $2p_{+1}$ state have been found to have a very similar shape, but with a most probable radius of around 200 Å.

3.4. Line shapes

It is interesting to note that most of the peaks in observed spectra of, for example, photoconductivity experiments, are asymmetric, having a sharp edge on the low-field side and spreading out much further to higher fields (see, for example, Grimes *et al* 1990). This shape can be predicted for transitions to hydrogenic states with predominantly even parity by looking at the effects of off-centre impurities for the hydrogenic states. All off-centre impurities are found to produce energy separations which are slightly less than those of the corresponding on-centre values at a given field, and thus equivalent energy gaps will occur at higher fields. This is independent of the sign of the displacement. Thus the peaks are due to on-centre impurities, with the net effects of off-centre impurities being to cause a broadening to the high-field side of the spectra only. The changes in energy separations are about 4 cm^{-1} for a 20 Å displacement and 20 cm^{-1} for a 50 Å displacement. For the 1s to $2p_{+1}$ transition, these will produce changes in the measured fields of about 0.3 and 1.3 T respectively. This is consistent with the widths observed experimentally for samples doped across the central 50 Å. A similar situation is likely to occur for transitions to metastable states. The shape of transitions to predominantly odd-parity states will be somewhat different, having a peak at some finite value of z_1, which will depend on the distribution of impurities in the sample, and therefore be at least weakly sample-dependent. Unfortunately, all transitions to such states observed so far are too weak to be able to determine any useful information in this respect.

4. Discussion

In this paper, the available experimental data for 150 Å wide wells have been explained successfully using a 3D hydrogenic model. However, the possibility that a quasi-2D model is also appropriate can not be entirely ruled out, as the patterns of observable transitions predicted on both models are very similar. This can be seen by comparing, for example, figure 4 of MacDonald and Ritchie (1986) and figure 2 of Wagner and Prettl (1988). Even though there are many more transitions possible in the bulk, there is a low probability of transition to the extra levels, making deductions from the experimental data inconclusive.

The biggest difference between the two approaches as far as the observable transitions are concerned is in the labelling of the states. The appropriate high-field labels on a 2D picture are simply (N, m), which are identical to the 3D labels with the quantum number ν fixed to be 0, subject to the extra condition that $m = \pm 1$ only. Thus a state labelled $(N, m, 0)$ in 3D becomes (N, m) in 2D. However, the labels indicating the weak-field parentage of the states are very different on the two pictures. In particular, all states in the 2D picture have a low-field counterpart, and so metastable states do not exist. For example, the $(1, \bar{1})$ state is associated with $3p_{-1}$ in 2D, but the $(1, \bar{1}, 0)$ state is metastable in 3D, with $3p_{-1}$ being associated with the $(0, \bar{1}, 2)$ 'hydrogenic' state.

Experimental evidence against a 2D picture are the points observed between $2p_{+1}$ and $2p_{-1}$, and the points tentatively identified with $3p_{+1} \equiv (1, 1, 2)$ in 3D notation. No levels are allowed between $(0, \bar{1})$ and $(1, 1)$ or between $(1, \bar{1})$ and $(2, 1)$ in 2D. However, the possibility of other origins for these points can not be entirely ruled out. In the 2D limit, the separations of the states $(N, 1, 0)$ and $(N + 1, 1, 0)$ are slightly larger than for the bulk equivalents. Unfortunately, the experimental data at present is not accurate enough to use these splittings to determine whether the system equates most closely to 2D or 3D. From a theoretical point of view, a 2D picture does not seem likely for 150 Å wide samples, as the effective Bohr radius (98.7 Å) is of the same order of magnitude as the well width. The 2D model will become more appropriate for much smaller well widths. Further experimental investigations are necessary to resolve the above questions.

Chang *et al* (1988) corrected the theoretical calculations of Greene and Lane (1986) for non-parabolicity and anisotropic effects in the conduction band of GaAs in order to fit their experimental data using the work of Zawadzki *et al* (1985) and Sigg *et al* (1987). These authors use a five-level $\boldsymbol{k} \cdot \boldsymbol{p}$ model in which the conduction and valence bands are split by spin–orbit coupling. This allows the cyclotron resonance effective mass of GaAs to be determined. However, they admit that the anisotropy of the effective mass is not very well reproduced by this model, and that the inclusion of more anisotropic interactions other than the band edge non-parabolicity are necessary. Also, it does not allow for any additional anisotropy introduced in the MQW case as compared with in the bulk. Hence the parallel and perpendicular masses have been treated as free parameters in our model. However, the final estimates for 150 Å wide wells are very close to the theoretically-predicted results of Ekenberg (1987), who obtained $m_{\parallel} = 0.069$ and $m_{\perp} = 0.067$ for this well width.

The positions of further hydrogenic and metastable states could be predicted using combinations of the methods used in the previous sections. It is also possible to predict lines using the empirical expression of Canuto and Kelly (1972) and Klaassen (1991) which deduce that the differences in energy between a Landau level N and the hydrogenic states (N, N, ν) are approximately proportional to $[(1 + \nu)/2]^{-2}$ for odd-parity states

and $(1 + \nu/2 + \delta)^{-2}$ for even parity states, where δ is the so-called quantum defect. However, the new states predicted in this manner do not fit any of the currently available experimental data. Hence, these results have not been presented here. Likewise, with the accuracy of the results at present, it has not been considered necessary to include central cell corrections and polaron effects in the model at this stage. These effects could be included in future work.

5. Summary

By combining the results of a theoretical model for hydrogenic impurities and knowledge of metastable states in the bulk, it has been possible to explain almost all of the recent FIR photoconductivity results of Grimes *et al* (1990) in terms of transitions from the 1s-like ground state of a hydrogenic impurity.

It was necessary to extend previous theories of hydrogenic impurities to include the effects of higher excited states, such as those with $m = 2$, and to allow mixing between odd and even parity states for impurities not located at the centre of a quantum well. A non-isotropic effective mass was also introduced into the model in order to improve the fit to the experimental data. This indicates that an effective parallel effective mass that is slightly larger than that for motion in the perpendicular direction should be used.

The states were then labelled according to their high-field counterparts, and a check was made that the states had the appropriate number of nodes along the z-direction by analyzing the shape of the predicted eigenstates. Metastable states were identified by extrapolating from the hydrogenic results, using known relationships between the energies of metastable states and knowledge of their relative energies in the bulk.

Results of the theoretical model indicate that transitions to states with $m = 2$ and to odd-parity states may be weakly observed. This is probably due to weak perturbations, such as electric field effects, and the mixings between odd and even parity states which must occur for off-centre impurities. Further work is necessary of both an experimental and a theoretical nature to conclusively identify some of the higher-energy states.

Acknowledgments

We are grateful to our colleagues Dr J M Chamberlain, Dr R Grimes and Dr M Stanaway at Nottingham University for alerting us to this problem and giving us the results of their experiments prior to publication. We would also like to thank Professor C A Bates for many helpful discussions. One of us (EP) wishes to thank the Science and Engineering Research Council for a Research Studentship.

References

Canuto V and Kelly D C 1972 *Astrophys. Space Sci.* **17** 277–91

Chang Y-H, McCombe B D, Mercy J-M, Reeder A A, Ralston J and Wicks G A 1988 *Phys. Rev. Lett.* **61** 1408–11

Cheng J-P, Li W J and McCombe B D 1990 *Mater. Sci. Forum* **65–6** 99–104

Cheng J-P and McCombe B D 1990 *Phys. Rev.* B **42** 7626–9

Dunn J L, Pearl E, Grimes R T, Stanaway M B and Chamberlain J M 1990 *Mater. Sci. Forum* **65–6** 117–22

Ekenberg U 1987 *Phys. Rev.* B **36** 6152–5

Fraizzoli S, Bassani F and Buczko R 1990 *Phys. Rev.* B **41** 5096–103
Greene R L and Bajaj K K 1985 *Phys. Rev.* B **31** 913–8
Greene R L and Lane P 1986 *Phys. Rev.* B **34** 8639–43
Grimes R T, Stanaway M B, Chamberlain J M, Dunn J L, Henini M, Hughes O H and Hill G 1990 *Semicond. Sci. Technol.* **5** 305–7
Hasegawa H and Howard R E 1961 *J. Phys. Chem. Solids* **21** 179–98
Huzinaga S 1965 *J. Chem. Phys.* **42** 1293–302
Jarosik N C, McCombe B D, Shanabrook B V, Comas J, Ralston J and Wicks G 1985 *Phys. Rev. Lett.* **54** 1283–6
Klaassen T O 1991 private communication
Lane P and Greene R L 1986 *Phys. Rev.* B **33** 5871–4
Lee H J, Juravel L Y, Wolley J C and Springthorpe A J 1980 *Phys. Rev.* B **21** 659–69
MacDonald A H and Ritchie D S 1986 *Phys. Rev.* B **33** 8336–44
Narita S and Miyao M 1971 *Solid State Commun.* **9** 2161–5
Sigg H, Perenboom J A A J, Pfeffer P and Zawadzki W 1987 *Solid State Commun.* **61** 685–9
Simola J and Virtamo J 1978 *J. Phys. B: At. Mol. Phys.* **11** 3309–22
Stillman G E, Larsen D M and Wolfe G M 1971 *Phys. Rev. Lett.* **27** 989–92
van Klarenbosch A, Klaassen T O, Wenckebach W Th and Foxon C T 1990 *J. Appl. Phys.* **67** 6323–8
Wagner H P and Prettl W 1988 *Solid State Commun.* **66** 367–9
Zawadzki W 1991 *Landau Level Spectroscopy* ed. G Landwehr and E I Rashba (Amsterdam: Elsevier) MPCMS 27.2, pp 1035–356
Zawadzki W, Pfeffer P and Sigg H 1985 *Solid State Commun.* **53** 777–82